



## Thermally enhanced blue light-emitting diode

Jin Xue, Yuji Zhao, Sang-Ho Oh, William F. Herrington, James S. Speck, Steven P. DenBaars, Shuji Nakamura, and Rajeev J. Ram

Citation: [Applied Physics Letters](#) **107**, 121109 (2015); doi: 10.1063/1.4931365

View online: <http://dx.doi.org/10.1063/1.4931365>

View Table of Contents: <http://scitation.aip.org/content/aip/journal/apl/107/12?ver=pdfcov>

Published by the [AIP Publishing](#)

---

### Articles you may be interested in

[Performance enhancement of blue light-emitting diodes with a special designed AlGaIn/GaN superlattice electron-blocking layer](#)

Appl. Phys. Lett. **99**, 221103 (2011); 10.1063/1.3653390

[Performance enhancement of blue light-emitting diodes with AlGaIn barriers and a special designed electron-blocking layer](#)

J. Appl. Phys. **110**, 093104 (2011); 10.1063/1.3651393

[Raman and emission characteristics of a-plane InGaIn/GaN blue-green light emitting diodes on r-sapphire substrates](#)

J. Appl. Phys. **109**, 043103 (2011); 10.1063/1.3549160

[Enhanced characteristics of blue In Ga N/Ga N light-emitting diodes by using selective activation to modulate the lateral current spreading length](#)

Appl. Phys. Lett. **92**, 261105 (2008); 10.1063/1.2953700

[Thermally stable and highly reflective AgAl alloy for enhancing light extraction efficiency in GaN light-emitting diodes](#)

Appl. Phys. Lett. **88**, 043507 (2006); 10.1063/1.2168264

---

The logo for AIP APL Photonics is displayed in white text on a red background. The letters 'AIP' are large and bold, followed by a vertical bar and the words 'APL Photonics' in a smaller font.

AIP | APL Photonics

*APL Photonics* is pleased to announce  
**Benjamin Eggleton** as its Editor-in-Chief



## Thermally enhanced blue light-emitting diode

Jin Xue,<sup>1</sup> Yuji Zhao,<sup>2</sup> Sang-Ho Oh,<sup>2</sup> William F. Herrington,<sup>1</sup> James S. Speck,<sup>3</sup> Steven P. DenBaars,<sup>2,3</sup> Shuji Nakamura,<sup>2,3</sup> and Rajeev J. Ram<sup>1,a)</sup>

<sup>1</sup>Department of Electrical Engineering and Computer Science, Massachusetts Institute of Technology, Cambridge, Massachusetts 02139, USA

<sup>2</sup>Department of Electrical and Computer Engineering, University of California, Santa Barbara, California 93106, USA

<sup>3</sup>Materials Department, University of California, Santa Barbara, California 93106, USA

(Received 22 June 2015; accepted 7 September 2015; published online 24 September 2015)

We investigate thermoelectric pumping in wide-bandgap GaN based light-emitting diodes (LEDs) to take advantage of high junction temperature rather than avoiding the problem of temperature-induced efficiency droop through external cooling. We experimentally demonstrate a thermally enhanced 450 nm GaN LED, in which nearly fourfold light output power is achieved at 615 K (compared to 295 K room temperature operation), with nearly no reduction in the wall-plug efficiency (i.e., electrical-optical energy conversion efficiency) at bias  $V < \hbar\omega/q$ . The LED is shown to work in a mode similar to a thermodynamic heat engine operating with charged carriers pumped into the active region by a combination of electrical work and Peltier heat (phonons) drawn from the lattice. In this optimal operating regime at 615 K, the LED injection current (3.26 A/cm<sup>2</sup>) is of similar magnitude to the operating point of common high power GaN based LEDs (5–35 A/cm<sup>2</sup>). This result suggests the possibility of removing bulky heat sinks in current high power LED products thus realizing a significant cost reduction for solid-state lighting. © 2015 AIP Publishing LLC. [<http://dx.doi.org/10.1063/1.4931365>]

A major driver for the mass production and deployment of light emitting diodes (LEDs) has been the rise in maximum achievable wall-plug efficiency (WPE)—defined as the ratio of the output optical power and the input electrical power. The lifetime cost of an LED is dominated by the operating cost which is inversely proportional to the wall-plug efficiency.<sup>1</sup> Intensive research into efficient visible LEDs has recently produced white light sources with luminous efficacy of 249 lm/W (Ref. 2) and is approaching the conventional limit imposed by the spectral requirements of general-purpose lighting and the electrical-to-optical power conversion efficiency limit of 100%. However, this power conversion limit fails to consider the entropy associated with the photons emerging from the LED.<sup>3</sup> The presence of entropy in incoherent electromagnetic radiation opens the possibility of providing heat as an input to the LED. As early as 1951, Lehovec *et al.* speculated on the role of thermoelectric heat exchange in SiC LEDs.<sup>4</sup> The authors were motivated by their observation of light emission with photon energy  $\hbar\omega$  ( $\lambda \approx 550$  nm) on the order of the electrical input energy per electron, given by the product of the electron's charge  $q$  and the bias voltage  $V$ . Then beginning with Jan Tauc in 1957,<sup>5</sup> a body of literature theoretically establishing the thermodynamic consistency of electro-luminescent cooling and exploring its limits began to emerge.<sup>6–9</sup> Recently, electroluminescent cooling was experimentally observed in an infrared LED based on InGaAsSb material system at very low bias ( $V < kT/q$ ).<sup>10,11</sup> Although the net cooling power and light output power (LOP) are still low at the bias level demonstrated due to low internal quantum efficiency (IQE),

this idea of thermoelectric pumping could be practically useful for real LED applications.

The ratio  $\hbar\omega/qV$  is the electrical-optical energy conversion efficiency for a single photon emission event, where  $\hbar\omega$  is photon energy,  $q$  is unit charge, and  $V$  is bias voltage. The ensemble WPE ( $\eta_{WP}$ ) for an LED includes the additional factor  $\eta_{EQE}$  describing the photon emission probability

$$\eta_{wp} = \frac{\hbar\omega}{qV} \times \eta_{EQE}. \quad (1)$$

$\eta_{EQE}$  has the maximum value of unity and is commonly known as the external quantum efficiency (EQE) of LEDs. Here, it is defined to include electrical injection efficiency and light extraction efficiency, as well as IQE.

Conventionally, high output powers for III-Nitride LEDs are achieved under high forward bias  $qV > \hbar\omega$  in a passively cooled ambient. However, these widely used nitride LEDs inevitably exhibit IQE degradation (thus EQE and WPE) at high current densities with the production of excessive heat. The increased junction temperature further reduces IQE and output power. These well-known current induced and temperature induced efficiency droop phenomena have hampered the further enhancement of III-Nitride high power LEDs and imposed additional cost on the heat sink.<sup>12,13</sup> In recent years, the dominant mechanisms of current induced efficiency droop, including Auger recombination, carrier leakage, density activated defect recombination, etc., have been extensively studied,<sup>12,14–21</sup> and remedies have been considered.<sup>21–27</sup> However, a comprehensive study and solution to the temperature induced efficiency droop (or thermal droop) was not reported.

<sup>a)</sup>E-mail: rajeev@mit.edu

In this letter, we investigate the possibility of thermoelectric pumping in wide-bandgap GaN based LEDs to take advantage of high junction temperature rather than avoiding the problem of thermal droop through external cooling. We experimentally demonstrate a thermally enhanced 450 nm high power GaN LED, in which a nearly fourfold enhancement in light output power is achieved at 615 K (compared to 295 K room temperature operation), with virtually no reduction in the wall-plug efficiency. In this optimal operating regime at 615 K, the LED injection current ( $3.26 \text{ A/cm}^2$ ) is of similar magnitude to the operating point of common high power GaN based LEDs ( $5\text{--}35 \text{ A/cm}^2$ ). This result suggests the possibility of removing the bulky heat sinks in current commercial high power LED products, thus realizing significant cost reduction and improved design flexibility.

The LED's enhanced high temperature performance is fundamentally attributed to thermoelectric pumping as the maximum WPE is observed at a bias  $V < \hbar\omega/q$ . In such a low bias regime, thermal excitation due to Peltier effect becomes necessary for a considerable amount of carrier injection. In other words, the LED works in a mode similar to a thermodynamic heat engine operating with charged carriers pumped into the active region by a combination of electrical work and Peltier heat (phonons) drawn from the lattice,<sup>28</sup> as depicted in Figure 1(a). The absorption of Peltier heat near junction area can be better understood from the perspective of statistical mechanics: only carriers at the high energy tail of Boltzmann distribution can be thermionically emitted above the diode's built-in potential barrier into the active region, with the remaining carriers absorbing heat from lattice (i.e., electron-phonon scattering) to restore the quasi-equilibrium distribution. If lattice temperature increases, carrier temperature also increases and thus the corresponding distribution profile moves towards higher energy. In this case, the thermionic emission can happen more easily, and the Peltier effect is more conspicuous. However, it is notable that, although the thermoelectric pumping mechanism introduces an additional pathway of input energy, the improvement of LED WPE at the low bias, high temperature regime is still conditional since fewer

injected carriers result in radiative recombination. Therefore, to realize an effective thermal enhancement of the LED performance at the proposed operation regime, the maintenance of a relatively high device IQE is a necessary condition, which requires low thermal droop as well as low current droop.

According to the standard rate equation model, the internal quantum efficiency of an LED can be written as

$$\eta_{IQE} = \frac{BN^2}{AN + BN^2 + CN^3}, \quad (2)$$

where  $N$  is the carrier density in the LED quantum well (QW) active region, and  $A$ ,  $B$ ,  $C$  are the associated Shockley-Read-Hall (SRH), radiative, and Auger recombination coefficients, respectively. The  $B$  and  $C$  coefficients scale with the magnitude of the overlap of the electron and hole wavefunctions:<sup>29</sup> Here, we investigate the optimization of the quantum efficiency at low-bias ( $V < \hbar\omega/q$ ) condition in which the Auger recombination is not dominant. Hence, we focus on maximizing the radiative bimolecular recombination ( $B$ ) while minimizing the non-radiative SRH recombination process. Both of these goals are achieved by growing the LED structure on a free-standing semi-polar GaN substrate.

For conventional GaN based heterostructure LEDs grown on c-plane sapphire substrates, the [0001] growth direction inherently results in a large discontinuity of piezoelectric polarization density in the GaN/InGaN/GaN QW active region. The polarization discontinuity then induces an internal electrical field  $\varepsilon_{pz}$  across the QW region, which is anti-parallel but much larger than the built-in field  $\varepsilon_{bi}$  of an LED junction. This strong net field causes the band structure to tilt in the QW region, displaces the electron and hole wavefunctions to opposite sides of the well, and leads to a significant reduction of wavefunction overlap.<sup>27</sup> For the sample studied in this work, however, this effect is largely mitigated through engineering the strength of  $\varepsilon_{pz}$ , i.e., growing LED in semi-polar  $[20\bar{2}1]$  direction to reduce  $\varepsilon_{pz}$  and make it partially cancel with  $\varepsilon_{bi}$  under low-bias operating conditions. In this case, the wavefunction overlap is maximized in the flat QW region and hence the radiative

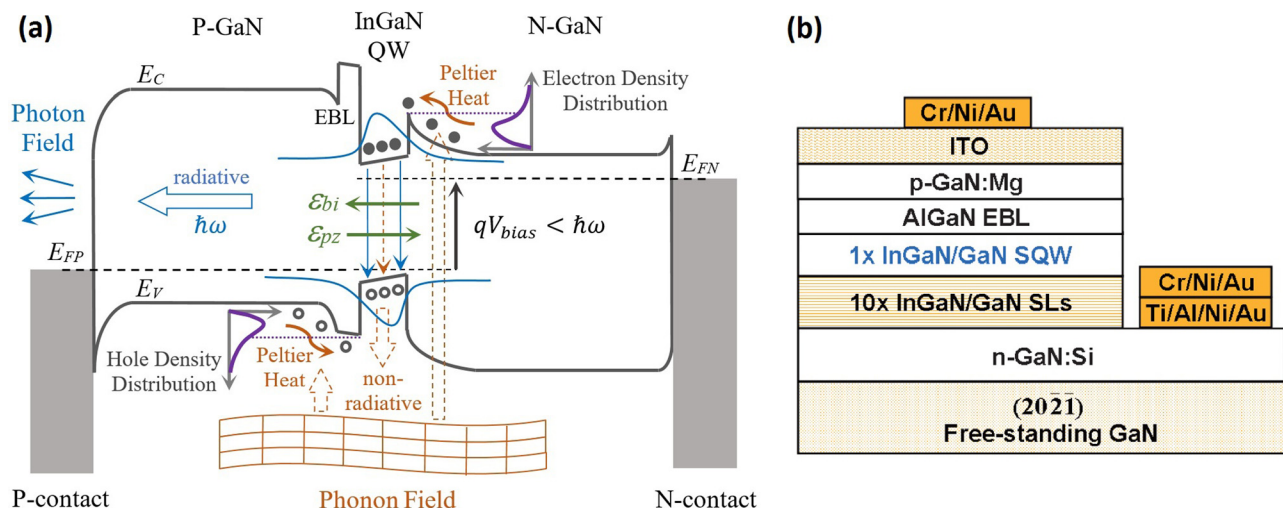


FIG. 1. (a) Band diagram of the InGaN single-quantum-well LED studied, the mechanism of thermoelectric pumping is also illustrated. (b) Epitaxial structure of the same sample device.



recombination rate is high (large B coefficient). The corresponding band structure of the sample studied is depicted in Figure 1(a). Band tilting is exaggerated to illustrate the effect of field in typical GaN based LEDs. For conventional GaN LEDs grown on c-plane sapphire substrates, the defect (mainly threading dislocation) density is on the order of  $10^8 \text{ cm}^{-2}$ ,<sup>30</sup> while this value can be as low as  $10^5 \text{ cm}^{-2}$  for those directly grown on free-standing GaN substrates.<sup>25</sup> Therefore, the high-quality growth of the LED active region on a free-standing semi-polar GaN substrate offers the possibility of reducing defect associated SRH recombination rate, while the improved wavefunction overlap increases the radiative recombination rate.

In the present work, a 450 nm small area ( $0.1 \text{ mm}^2$ ) InGaN single-quantum-well LED specifically designed for high power and low current-induced efficiency droop is studied. The epitaxial structure of the sample device studied is shown in Figure 1(b).<sup>25</sup> It consists of an n-type GaN layer ( $1 \mu\text{m}$  thick with Si doping concentration of  $1 \times 10^{19} \text{ cm}^{-3}$ ), followed by 10 pairs of  $\text{In}_{0.01}\text{Ga}_{0.99}\text{N}/\text{GaN}$  (3/3 nm) undoped buffer layers, a  $\text{GaN}/\text{In}_{0.18}\text{Ga}_{0.82}\text{N}/\text{GaN}$  single QW (10 nm GaN bottom barrier, 12 nm InGaN QW and 15 nm GaN upper barrier), a  $\text{Al}_{0.18}\text{Ga}_{0.82}\text{N}$  electron blocking layer (EBL, 3 nm with Mg doping concentration of  $2 \times 10^{19} \text{ cm}^{-3}$ ), and a p-type GaN layer (50 nm with Mg doping concentration of  $4 \times 10^{19} \text{ cm}^{-3}$ ). Through the approach of high-quality semi-polar growth on GaN substrate, this high power LED exhibits its low current induced efficiency droop as expected. An encapsulated sample with backside roughening and a ZnO vertical-stand package has an EQE of 50.1% and a LOP of 140 mW at  $100 \text{ A/cm}^2$ .<sup>25</sup> To facilitate experiments over a wide temperature range, the LEDs tested were bare dies without packaging or encapsulation, resulting in lower EQE and WPE measurement values than devices optimized for high light extraction.<sup>31</sup> A schematic of the experimental setup is shown in the inset of Figure 2. During the testing, an LED die (approximately 5 mm by mm) is placed on the plane surface of a hemispherical sapphire solid-immersion lens (10 mm in diameter) for probing. The hemisphere is anti-reflection coated sapphire to approximately match the index of GaN substrate and has relatively high thermal conductivity. The sapphire lens sits in an opening of a copper arm that can be heated. Multiple thermocouples are attached to the

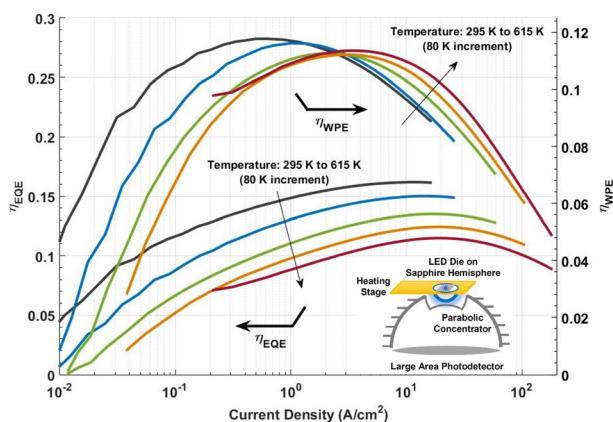


FIG. 2. EQE and WPE versus LED current density at different temperatures. A schematic of the experimental setup is shown in the inset.

sapphire lens and the copper arm to monitor the temperature. A compound parabolic concentrator is placed a few millimeters underneath the sapphire lens with a large area ( $613.0 \text{ mm}^2$ ), calibrated silicon photo detector in the bottom for maximum light collection. In our measurements, pulse-mode voltage sweeps were performed from 2 to 5 V under ambient temperatures of 295 K, 375 K, 455 K, 535 K, and 615 K, respectively. Data are collected after the system reaches thermal equilibrium.

The dependence of EQE and WPE on LED current density at different temperatures is shown in Figure 2. As expected, EQE exhibits a small efficiency droop at high current density. It is notable that, although the peak EQE reduces with increasing temperature, the peak WPE has no significant drop. In fact, since the collection efficiency of the experimental setup is optimized at room temperature, thermal expansion of the heating stage relative to the photodetector is likely responsible for the small roll-off in the measured WPE at higher temperatures. The dependence of EQE and WPE on LED bias at different temperatures is also shown in Figure 3. It is observed that with the increase of temperature, peak WPE point gradually moves towards lower bias regime with virtually no reduction in value. As discussed in Equation (1), this is mainly because of the reduction in bias voltage, and more importantly for the minimal drop in EQE for large thermal excitation. A closer comparison for the two extreme cases at 295 K and 615 K is shown in Figure 4, with their corresponding LOP plotted together. As labelled in the figure, the bias voltage 3.35 V corresponding to peak WPE at 295 K has moved to 2.5 V at 615 K, with nearly fourfold increase in light output power and only 0.42% reduction in WPE (not calibrated for thermal expansion). The operating conditions for peak WPE at different temperatures are listed in Table I. It clearly tracks the continuous change of peak WPE and the corresponding EQE, indicating a growing LOP and reduced forward bias at higher temperatures. Note that the value of WPE starts to exceed EQE at 535 K, indicating the onset of low bias operation ( $V < \hbar\omega/q$ ) and effective thermoelectric pumping. In addition, the injection current density in the case of 615 K ( $3.26 \text{ A/cm}^2$ ) is already close to the value of  $5 \text{ A/cm}^2$ , which is the operating point of common high power GaN based LEDs.

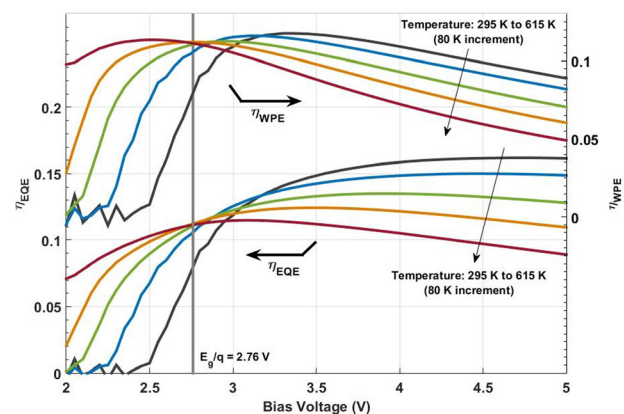


FIG. 3. EQE and WPE versus LED bias voltage at different temperatures. The bias voltage corresponding to the photon energy is indicated.

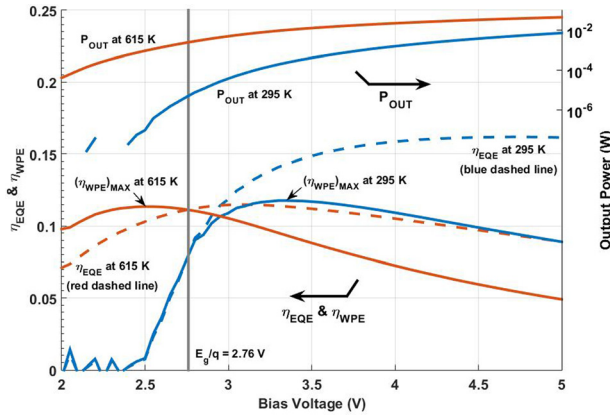


FIG. 4. EQE (dashed lines) and WPE (solid lines) versus LED bias voltage at two extreme temperatures cases. All blue lines correspond to 295 K room temperature operation, and red lines correspond to 615 K high temperature operation. The bias voltage corresponding to the photon energy is indicated.

To further look into the role that Peltier effect plays at different operation conditions, the total LED heating power (per unit area)  $Q_{total}$  generated from all sources including Peltier heating (intraband phonon emission or absorption)  $Q_{Peltier}$ , non-radiative carrier recombination  $Q_{non-rad}$ , and Joule heating  $Q_{Joule}$  arising from series resistance can be analyzed and expressed as

$$Q_{total} = Q_{Peltier} + Q_{non-rad} + Q_{Joule} = JV \times (1 - \eta_{WPE}), \quad (3)$$

where  $J$  is the injection current density of LED. An approximate magnitude for the Peltier heating component  $Q_{Peltier}$  can be determined from

$$Q_{Peltier} = \left( V - IR_s - \frac{\hbar\omega}{q} \right) \times J, \quad (4)$$

where  $R_s$  is the total series resistance of LED. It can be observed that the total heating power  $Q_{total}$  is always a positive so long as the wall-plug efficiency is below 100%, while the total Peltier heating component could become negative at low bias regime ( $V < \hbar\omega/q$ ), indicating a transition from Peltier heating to Peltier cooling. For instance, a plot of  $Q_{total}$  and  $Q_{Peltier}$  versus LED bias at 295 K and 615 K is shown in Figure 5. A clear comparison in the relative magnitude of Peltier cooling power for the two temperature cases shows its dependence on the junction temperature: the Peltier effect is greatly enhanced at larger thermal excitation (i.e., higher junction temperature), mainly due to the exponential increase of injection current, according to Equation (4). The Peltier heating power (per unit area) for peak WPE operation at different temperatures is also listed in Table I.

TABLE I. Conditions of reaching peak WPE at different temperatures.

T (K)	V (V)	J (A/cm <sup>2</sup> )	P <sub>OUT</sub> at Max WPE (W/cm <sup>2</sup> )	$\eta_{EQE}$ (%)	$\eta_{WP\_MAX}$ (%)	$Q_{Peltier}$ (W/cm <sup>2</sup> )
295	3.35	0.61	2.40	14.31	11.77	$3.46 \times 10^{-1}$
375	3.10	1.00	3.61	13.07	11.61	$3.12 \times 10^{-1}$
455	2.95	2.11	7.01	12.06	11.26	$3.43 \times 10^{-1}$
535	2.75	2.94	9.06	11.19	11.21	$-9.83 \times 10^{-2}$
615	2.50	3.26	9.24	10.30	11.35	$-9.02 \times 10^{-1}$

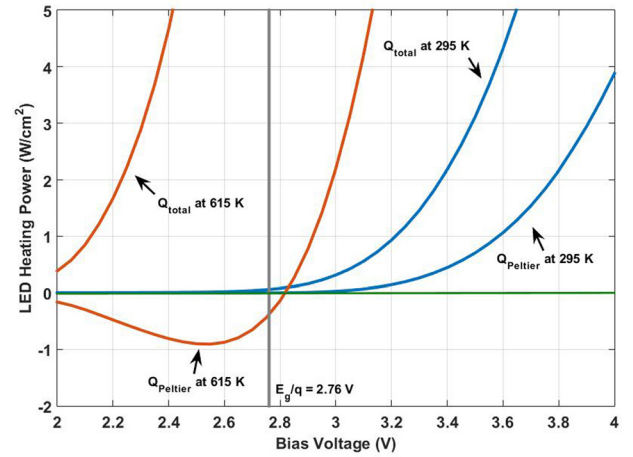


FIG. 5. Total LED heating power  $Q_{total}$  and the Peltier heating component  $Q_{Peltier}$  versus LED bias voltage at two extreme temperature cases. All blue lines correspond to 295 K room temperature operation, and red lines correspond to 615 K high temperature operation. The bias voltage corresponding to the photon energy is indicated.

Again the change of sign of these values indicates the initiation of effective thermoelectric pumping above 535 K.

This low bias optimal regime of high LOP and high WPE at elevated temperature does not universally exist for common GaN based LEDs. The demonstration of the sample studied is attributed to the low current droop and low thermal droop for the EQE in this device. To achieve low thermal droop, reducing the density of defect states in LEDs is crucial, as the trap assisted SRH non-radiative recombination dominates the temperature dependence at low-bias.<sup>30</sup> By assuming that traps capture electrons and holes at the same rate, the SRH recombination lifetime has approximately the following temperature dependence:<sup>32</sup>

$$\tau_{SRH} = \tau_0 \left( 1 + \cosh \frac{E_{Trap} - E_{Fi}}{kT} \right), \quad (5)$$

where  $\tau_0$  is a constant dependent on defect density and carrier capture rates. Increasing the density of defect states results in smaller  $\tau_0$ .  $E_{Trap}$  and  $E_{Fi}$  are the trap energy level and intrinsic Fermi level within the energy bandgap, respectively. According to the temperature dependence of Equation (5), we can see that a higher temperature LED junction results in an exponentially shorter SRH lifetime and thus a lower IQE.

An empirical relation describing LED light output power at different temperatures (for a constant current density) is given by<sup>30</sup>

$$P_{OUT}(T) = P_{OUT\_300K} \times \exp\left(-\frac{T - 300K}{T_C}\right), \quad (6)$$

where  $T_C$  is the device characteristic temperature, with higher value indicating better thermal droop performance. At a current density around 10 A/cm<sup>2</sup>, compared to the  $T_C$  values of less than 200 K for typical GaN based LEDs grown on c-plane sapphire substrates,<sup>30</sup> the samples we studied here exhibit a much higher value of 869 K, indicating a lower decay rate in IQE with increasing temperature, which is likely due to the reduced defect density in the LED active region.

In summary, by taking advantage of thermoelectric pumping, we demonstrate a thermally enhanced 450 nm high power GaN LED, in which nearly fourfold LOP is achieved at 615 K (compared to 295 K room temperature operation), with nearly no reduction in the wall-plug efficiency. Under this 615 K maximum WPE operation condition at  $V < \hbar\omega/q$ , the LED injection current ( $3.26 \text{ A/cm}^2$ ) is found to be close to the value of  $5 \text{ A/cm}^2$ , which is the operating point of common high power GaN based LEDs. This result suggests the possibility of removing bulky heat sinks in commercial high power LED products, bringing a considerable reduction in the cost for general illumination.

This work was supported by Professor Amar G. Bose Research Grants and fellowship from Agency for Science, Technology and Research (A\*STAR), Singapore. The work at UCSB was supported by the Solid State Lighting and Energy Electronics Center (SSLEEC). The authors would like to thank Parthiban Santhanam for having worked on the initial thermodynamic calculations of white light LEDs that helped motivate this work. The authors also thank Professor Claude Weisbuch for useful discussions.

- <sup>1</sup>Technology Focus, "LEDs and their applications," *Nat. Photonics* **1**, 23 (2007).
- <sup>2</sup>Y. Narukawa, M. Ichikawa, D. Sanga, M. Sano, and T. Mukai, "White light emitting diodes with super-high luminous efficacy," *J. Phys. D: Appl. Phys.* **43**(35), 354002 (2010).
- <sup>3</sup>M. A. Weinstein, "Thermodynamic limitation on the conversion of heat into light," *J. Opt. Soc. Am.* **50**(6), 597–602 (1960).
- <sup>4</sup>K. Lehovc, C. A. Accardo, and E. Jamgochian, "Injected light emission of silicon carbide crystals," *Phys. Rev.* **83**(3), 603–607 (1951).
- <sup>5</sup>J. Tauc, "The share of thermal energy taken from the surroundings in the electro-luminescent energy radiated from a p-n junction," *Czech. J. Phys.* **7**, 275–276 (1957).
- <sup>6</sup>P. T. Landsberg and D. A. Evans, "Thermodynamic limits for some light-producing devices," *Phys. Rev.* **166**, 242 (1968).
- <sup>7</sup>P. T. Landsberg and G. Tonge, "Thermodynamic energy conversion efficiencies," *J. Appl. Phys.* **51**, R1 (1980).
- <sup>8</sup>P. Berdahl, "Radiant refrigeration by semiconductor diodes," *J. Appl. Phys.* **58**, 1369 (1985).
- <sup>9</sup>A. G. Mal'shukov and K. A. Chao, "Opto-thermionic refrigeration in semiconductor heterostructures," *Phys. Rev. Lett.* **86**, 5570 (2001).
- <sup>10</sup>P. Santhanam, D. J. Gray, Jr., and R. J. Ram, "Thermoelectrically pumped light-emitting diodes operating above unity efficiency," *Phys. Rev. Lett.* **108**, 097403 (2012).
- <sup>11</sup>P. Santhanam, D. Huang, R. J. Ram, M. A. Remennyi, and B. A. Matveev, "Room temperature thermo-electric pumping in mid-infrared light-emitting diodes," *Appl. Phys. Lett.* **103**, 183513 (2013).
- <sup>12</sup>J. Piprek, "Efficiency droop in nitride-based light-emitting diodes," *Phys. Status Solidi A* **207**(10), 2217–2225 (2010).
- <sup>13</sup>D. S. Meyaard, Q. Shan, J. Cho, E. F. Schubert, S. H. Han, M. H. Kim, C. Sone, S. J. Oh, and J. K. Kim, "Temperature dependent efficiency droop in GaInN light-emitting diodes with different current densities," *Appl. Phys. Lett.* **100**, 081106 (2012).
- <sup>14</sup>M. H. Kim, M. F. Schubert, Q. Dai, J. K. Kim, E. Fred Schubert, J. Piprek, and Y. Park, "Origin of efficiency droop in GaN-based light-emitting diodes," *Appl. Phys. Lett.* **91**, 183507 (2007).

- <sup>15</sup>A. David and M. J. Grundmann, "Droop in InGaN light-emitting diodes: A differential carrier lifetime analysis," *Appl. Phys. Lett.* **96**, 103504 (2010).
- <sup>16</sup>J. Hader, J. V. Moloney, and S. W. Koch, "Temperature-dependence of the internal efficiency droop in GaN-based diodes," *Appl. Phys. Lett.* **99**, 181127 (2011).
- <sup>17</sup>D. S. Meyaard, Q. Shan, Q. Dai, J. Cho, E. F. Schubert, M. H. Kim, and C. Sone, "On the temperature dependence of electron leakage from the active region of GaInN/GaN light-emitting diodes," *Appl. Phys. Lett.* **99**, 041112 (2011).
- <sup>18</sup>D. S. Meyaard, G. B. Lin, Q. Shan, J. Cho, E. F. Schubert, H. Shim, M. H. Kim, and C. Sone, "Asymmetry of carrier transport leading to efficiency droop in GaInN based light-emitting diodes," *Appl. Phys. Lett.* **99**, 251115 (2011).
- <sup>19</sup>J. Iveland, L. Martinelli, J. Peretti, J. S. Speck, and C. Weisbuch, "Direct measurement of auger electrons emitted from a semiconductor light-emitting diode under electrical injection: Identification of the dominant mechanism for efficiency droop," *Phys. Rev. Lett.* **110**, 177406 (2013).
- <sup>20</sup>D. S. Meyaard, G. B. Lin, J. Cho, E. F. Schubert, H. Shim, S. H. Han, M. H. Kim, C. Sone, and Y. S. Kim, "Identifying the cause of the efficiency droop in GaInN light-emitting diodes by correlating the onset of high injection with the onset of the efficiency droop," *Appl. Phys. Lett.* **102**, 251114 (2013).
- <sup>21</sup>G. Verzellesi, D. Saguatti, M. Meneghini, F. Bertazzi, M. Goano, G. Meneghesso, and E. Zanoni, "Efficiency droop in InGaN/GaN blue light-emitting diodes: Physical mechanisms and remedies," *J. Appl. Phys.* **114**, 071101 (2013).
- <sup>22</sup>N. F. Gardner, G. O. Müller, Y. C. Shen, G. Chen, S. Watanabe, W. Götz, and M. R. Krames, "Blue-emitting InGaN-GaN double-heterostructure light-emitting diodes reaching maximum quantum efficiency above  $200 \text{ A/cm}^2$ ," *Appl. Phys. Lett.* **91**, 243506 (2007).
- <sup>23</sup>M. F. Schubert, J. Xu, J. K. Kim, E. F. Schubert, M. H. Kim, S. Yoon, S. M. Lee, C. Sone, T. Sakong, and Y. Park, "Polarization-matched GaInN/AlGaInN multi-quantum-well light-emitting diodes with reduced efficiency droop," *Appl. Phys. Lett.* **93**, 041102 (2008).
- <sup>24</sup>H. Zhao, G. Liu, J. Zhang, Jo. D. Poplawsky, V. Dierolf, and N. Tansu, "Approaches for high internal quantum efficiency green InGaN light-emitting diodes with large overlap quantum wells," *Opt. Express* **19**(104), A991–A1007 (2011).
- <sup>25</sup>C. C. Pan, S. Tanaka, F. Wu, Y. Zhao, J. S. Speck, S. Nakamura, S. P. DenBaars, and D. Feezell, "High-power, low-efficiency-droop semipolar  $[20\bar{2}1]$  single-quantum-well blue light-emitting diodes," *Appl. Phys. Express* **5**, 062103 (2012).
- <sup>26</sup>Y. Zhao, S. Tanaka, C. C. Pan, K. Fujito, D. Feezell, J. S. Speck, S. P. DenBaars, and S. Nakamura, "High-power blue-violet semipolar  $[20\bar{2}1]$  InGaN/GaN light-emitting diodes with low efficiency droop at  $200 \text{ A/cm}^2$ ," *Appl. Phys. Express* **4**, 082104 (2011).
- <sup>27</sup>D. F. Feezell, J. S. Speck, S. P. DenBaars, and S. Nakamura, "Semipolar  $[20\bar{2}1]$  InGaN/GaN light-emitting diodes for high-efficiency solid-state lighting," *J. Disp. Technol.* **9**(4), 190–198 (2013).
- <sup>28</sup>K. P. Pipe, R. J. Ram, and A. Shakouri, "Bias-dependent Peltier coefficient and internal cooling in bipolar devices," *Phys. Rev. B* **66**, 125316 (2002).
- <sup>29</sup>L. A. Coldren, S. W. Crozine, and M. L. Masanovic, *Diode Lasers and Photonic Integrated Circuits* (Wiley, Hoboken, NJ, USA, 2012), pp. 158–186.
- <sup>30</sup>S. Chhajed, J. Cho, E. F. Schubert, J. K. Kim, D. D. Koleske, and M. H. Crawford, "Temperature-dependent light-output characteristics of GaInN light-emitting diodes with different dislocation densities," *Phys. Status Solidi A* **208**, 947 (2011).
- <sup>31</sup>C. A. Humi, A. David, M. J. Cich, R. I. Aldaz, B. Ellis, K. Huang, A. Tyagi, R. A. DeLille, M. D. Craven, F. M. Steranka, and M. R. Krames, "Bulk GaN flip-chip violet light-emitting diodes with optimized efficiency for high-power operation," *Appl. Phys. Lett.* **106**, 031101 (2015).
- <sup>32</sup>E. F. Schubert, *Light-Emitting Diodes*, 2nd ed. (Cambridge University Press, Cambridge, 2006).